



Comparative Performance of Susceptibility Map-Weighted MRI According to the Acquisition Planes in the Diagnosis of Neurodegenerative Parkinsonism

Suiji Lee^{1*}, Chong Hyun Suh^{1*}, Sungyang Jo², Sun Ju Chung², Hwon Heo¹, Woo Hyun Shim¹, Jongho Lee³, Ho Sung Kim¹, Sang Joon Kim¹, Eung Yeop Kim⁴

¹Department of Radiology and Research Institute of Radiology, Asan Medical Center, University of Ulsan College of Medicine, Seoul, Republic of Korea

²Department of Neurology, Asan Medical Center, University of Ulsan College of Medicine, Seoul, Republic of Korea

³Department of Electrical and Computer Engineering, Seoul National University, Seoul, Republic of Korea

⁴Department of Radiology, Samsung Medical Center, Sungkyunkwan University School of Medicine, Seoul, Republic of Korea

Objective: To evaluate the diagnostic performance of susceptibility map-weighted imaging (SMwI) taken in different acquisition planes for discriminating patients with neurodegenerative parkinsonism from those without.

Materials and Methods: This retrospective, observational, single-institution study enrolled consecutive patients who visited movement disorder clinics and underwent brain MRI and ¹⁸F-FP-CIT PET between September 2021 and December 2021. SMwI images were acquired in both the oblique (perpendicular to the midbrain) and the anterior commissure-posterior commissure (AC-PC) planes. Hyperintensity in the substantia nigra was determined by two neuroradiologists. ¹⁸F-FP-CIT PET was used as the reference standard. Inter-rater agreement was assessed using Cohen's kappa coefficient. The diagnostic performance of SMwI in the two planes was analyzed separately for the right and left substantia nigra. Multivariable logistic regression analysis with generalized estimating equations was applied to compare the diagnostic performance of the two planes.

Results: In total, 194 patients were included, of whom 105 and 103 had positive results on ¹⁸F-FP-CIT PET in the left and right substantia nigra, respectively. Good inter-rater agreement in the oblique ($\kappa = 0.772/0.658$ for left/right) and AC-PC planes (0.730/0.741 for left/right) was confirmed. The pooled sensitivities for two readers were 86.4% (178/206, left) and 83.3% (175/210, right) in the oblique plane and 87.4% (180/206, left) and 87.6% (184/210, right) in the AC-PC plane. The pooled specificities for two readers were 83.5% (152/182, left) and 82.0% (146/178, right) in the oblique plane, and 83.5% (152/182, left) and 86.0% (153/178, right) in the AC-PC plane. There were no significant differences in the diagnostic performance between the two planes ($P > 0.05$).

Conclusion: There are no significant difference in the diagnostic performance of SMwI performed in the oblique and AC-PC plane in discriminating patients with parkinsonism from those without. This finding affirms that each institution may choose the imaging plane for SMwI according to their clinical settings.

Keywords: Primary parkinsonism; Magnetic resonance image; Susceptibility map-weighted imaging; Image plane

Received: September 19, 2023 **Revised:** December 3, 2023 **Accepted:** January 3, 2024

*These authors contributed equally to this work.

Corresponding author: Chong Hyun Suh, MD, Department of Radiology and Research Institute of Radiology, Asan Medical Center, University of Ulsan College of Medicine, 88 Olympic-ro 43-gil, Songpa-gu, Seoul 05505, Republic of Korea

• E-mail: chonghyunsuh@amc.seoul.kr

Corresponding author: Eung Yeop Kim, MD, Department of Radiology, Samsung Medical Center, Sungkyunkwan University School of Medicine, 81 Irwon-ro, Gangnam-gu, Seoul 06351, Republic of Korea

• E-mail: neuroradkim@gmail.com

This is an Open Access article distributed under the terms of the Creative Commons Attribution Non-Commercial License (<https://creativecommons.org/licenses/by-nc/4.0>) which permits unrestricted non-commercial use, distribution, and reproduction in any medium, provided the original work is properly cited.

INTRODUCTION

Idiopathic Parkinson's disease (IPD) is a neurodegenerative disorder characterized by the loss of dopaminergic neurons in the substantia nigra [1]. The diagnosis of IPD is generally based on clinical symptoms, and the International Parkinson and Movement Disorder Society has recently revised the diagnostic criteria to include dopamine transporter imaging, including N-3-fluoropropyl-2- β -carbomethoxy-3- β -(4-iodophenyl) nortropane (^{18}F -FP-CIT) PET as an exclusion criterion [2]. However, ^{18}F -FP-CIT PET lacks generalizability and cost-effectiveness in real-world settings.

Currently, high-resolution MRI is widely applied to diagnose IPD. Several studies have suggested that the loss of dorsolateral nigral hyperintensity on susceptibility-weighted imaging (SWI) (i.e., loss of the swallowtail appearance) indicates nigrostriatal dopaminergic degeneration and can thus be used as an imaging biomarker for IPD [3-7]. Furthermore, the visibility of the nigrosome 1 on MRI has been improved with "susceptibility map-weighted imaging (SMwI)," which resolves the blooming artifacts of SWI and improves the contrast-to-noise and signal-to-noise ratio [8-11] over SWI.

Prior studies have shown the high diagnostic performances of both SWI and SMwI in determining the nigral hyperintensity in the substantia nigra [3-18]. However, these studies used heterogeneous study populations and imaging protocols, and discretionally chose different types of MR acquisition planes. One recent pioneering study assessed the loss of nigral hyperintensity as a biomarker of IPD using a plane parallel to the splenium and genu lines of the corpus callosum [4]. Several studies have further implemented a plane perpendicular to the midbrain [8,12,19], whereas others adopted an anterior commissure-posterior commissure (AC-PC) plane as it is easy to conduct and shows little deviation in repeated trials [17]. However, in a recent meta-analysis, the perpendicular plane showed better diagnostic performance than the AC-PC plane, with a sensitivity of 0.94 (95% confidence interval [CI], 0.82-1.00) and a specificity of 0.98 (95% CI, 0.95-1.00) on the perpendicular plane and 0.76 (95% CI, 0.86-1.00) and a specificity of 0.95 (95% CI, 0.91-0.99) on the AC-PC plane. Meanwhile, several recent studies have used the oblique plane, suggesting that it can minimize the partial volume effect as it run perpendicular to the long axis of the dorsal substantia nigra [16,20,21]. However, the opinions of these

authors were somewhat speculative, and the studies were limited by a lack of direct comparison between the oblique plane and other MR acquisition planes.

To the best of our knowledge, no study has previously analyzed the performance of SMwI in assessing nigral hyperintensity according to the MR acquisition plane. Therefore, this study aimed to compare the diagnostic performance of oblique and AC-PC planes in assessing nigral hyperintensity and establish an optimized SMwI protocol for the diagnosis of primary parkinsonism.

MATERIALS AND METHODS

Patients and Clinical Assessment

This retrospective study was approved by the Institutional Review Board of Asan Medical Center (IRB No. 2021-1642), and was performed and reported for adherence to STARD 2015 [22]. This study included consecutive patients who visited the movement disorder clinics at Asan Medical Center and underwent brain MRI between September 2021 and December 2021. The exclusion criteria were as follows: 1) patients without ^{18}F -FP-CIT PET results, 2) ^{18}F -FP-CIT PET results acquired more than 1 year prior, 3) patients with symptom onset more than 5 years prior, 4) final diagnosis of vascular parkinsonism, 5) final diagnosis of secondary parkinsonism due to a tumor, 6) inconclusive diagnosis, and 7) poor image quality. Data were collected from the electronic medical records. Clinical diagnoses were made by a neurologist with 8 years of experience (S.Y.J.) in accordance with the respective clinical diagnostic criteria. Clinical diagnoses of IPD were made according to the UK Parkinson's Disease Society Brain Bank clinical diagnostic criteria, including bradykinesia and at least one symptom of muscular rigidity, resting tremor, postural instability, and other clinical findings [1]. Other diseases, including multiple system atrophy, progressive supranuclear palsy, corticobasal syndrome, and essential tremor, were diagnosed according to consensus diagnostic criteria [23-26].

Imaging Acquisition

Participants underwent brain MRI using a 3T scanner with a 32-channel coil, and ^{18}F -FP-CIT PET imaging of the brain was performed after the injection of 5 mCi (185 MBq) using a PET/CT scanner (Siemens Biograph TruePoint; 148 sections with a section thickness of 1.5 mm). SWI was obtained using a 3T MRI scanner (Ingenia CX; Philips, Best, Netherlands) with a 32-channel SENSE head coil (Philips Healthcare)

and 3D multi-echo gradient recalled echo sequence with the following parameters: shortest repeat time (TR); a total of three echoes; first echo time (TE), 14 msec; echo interval, 13 msec; flip angle, 20°; field of view (FOV), 192 x 192 mm²; voxel size, 0.5 x 0.5 x 1 mm²; and slice number, 32. The acquisition time for SMI was 4 minutes 53 seconds. After SWI acquisition, SMwI was performed to enhance the visibility of nigrosome 1. Post-processing and reconstruction of SMwI images were performed following a method previously reported by Nam et al. [9]. Channel-combined magnitude images were obtained, and the magnitude images of the six echoes were separated into a single image using the root sum of the squares of the multichannel magnitude images. The phase images were generated as a complex mean after adjusting for the global phase offsets of the individual images. Using the phase images of different TEs, frequency images were obtained using the unwarping algorithm. Subsequently, quantitative susceptibility mapping (QSM) was reconstructed and transformed to obtain a QSM mask. Finally, the SMwI image was obtained by accumulating the multiecho correlated magnitude images with the QSM mask. The reconstruction slice thickness of the SMwI was 1 mm. Two types of SMwIs with different planes were acquired: the AC-PC plane and the oblique coronal plane (Fig. 1). The AC-PC plane images were obtained parallel to the plane from the AC-PC. Oblique coronal planes were obtained as parallel planes from the PC to the anterosuperior border of the pons, approximately perpendicular to the midbrain.

Image Analysis

Two radiologists (C.H.S. and S.J.L., with 12 and 2 years of experience, respectively) underwent training sessions of 1 month for 50 cases with both AC-PC plane and oblique coronal plane images acquired between July 2021 and August 2021 from the Asan Medical Center. Subsequently, two readers independently evaluated the status of nigral hyperintensity in the bilateral substantia nigra of eligible patients, blinded to the clinical diagnoses and ¹⁸F-FP-CIT PET findings. These two readers separately evaluated the images at the dedicated stations, ensuring that their ratings were not affected by each other. First, only AC-PC plane images were presented during the first reading session. After a 2 month washout period, the second reading session started in the oblique coronal plane. The readers had no access to either plane for any patient.

The nigrosome 1 region on the oblique plane was defined as the hyperintense area immediately anterior to the inferior portion of the red nucleus, which was visualized between the curvilinear hypointense areas, while the nigrosome 1 region on the AC-PC plane was defined as the hyperintense area immediately posterior to the inferior portion of the red nucleus (Fig. 2) [20]. Abnormalities were determined when any hypointense area obliterated the differentiation of the three layers (the inner, middle, and outer hypointense layers) [16]. Each side of the substantia nigra was assessed separately and classified into three categories: Category 2 was “absolutely abnormal,” indicating complete obliteration

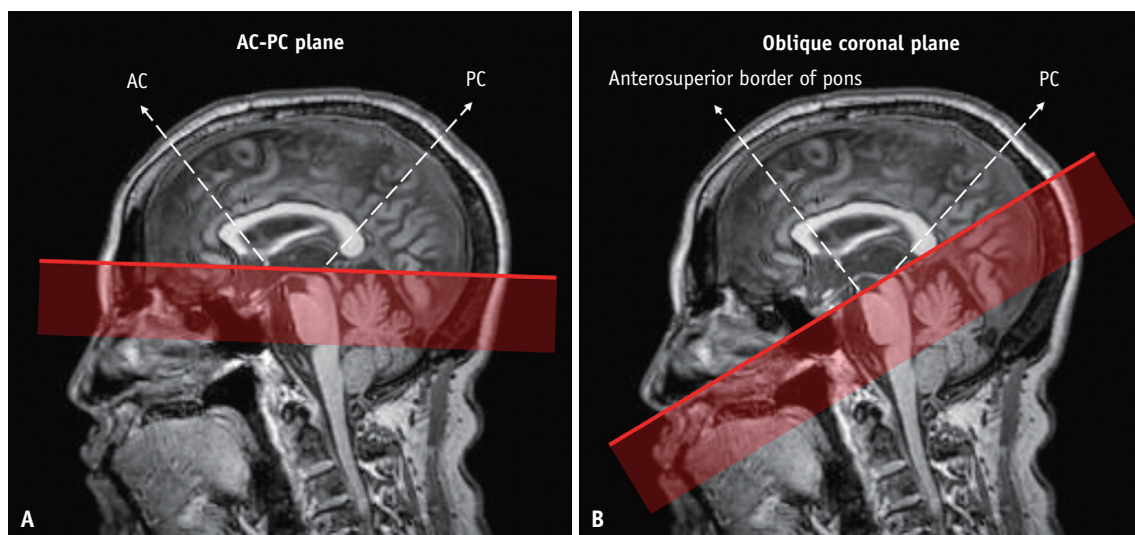


Fig. 1. AC-PC plane images were obtained parallel to the plane from the AC-PC. Oblique coronal planes were further obtained as a parallel plane from the PC to the anterosuperior border of the pons, approximately perpendicular to the midbrain. AC = anterior commissure, PC = posterior commissure

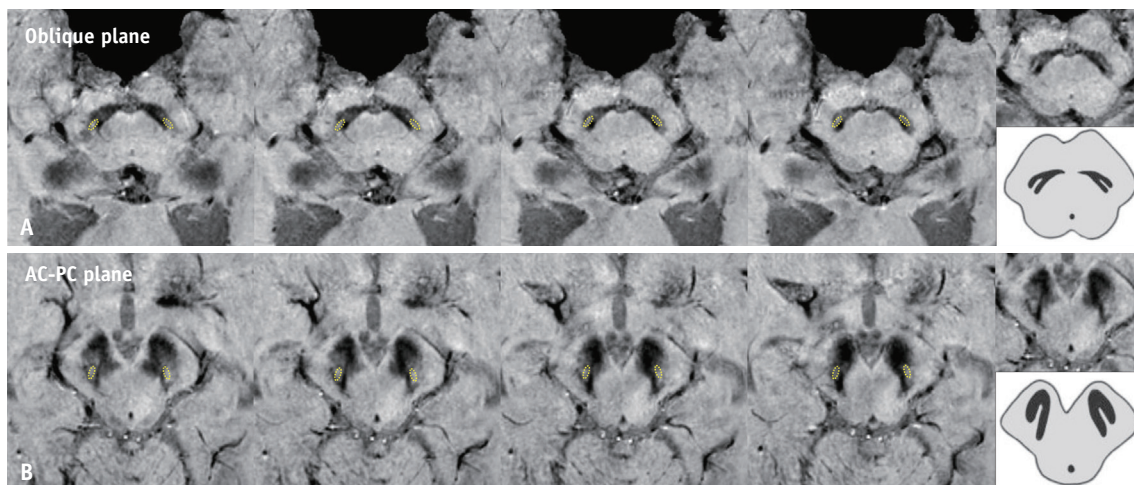


Fig. 2. The nigrosome 1 region in this study was defined as the hyperintense area located immediately anterior to the inferior portion of the red nucleus, visualized between the curvilinear hypointense areas. From the point when the red nucleus disappears (the first images in the oblique plane and AC-PC plane), the four consecutive 1-mm resliced images below the red nucleus were selected for visual analysis. The yellow dotted lines indicate the normal nigrosome 1 regions in (A) the oblique and (B) AC-PC planes, respectively. AC = anterior commissure, PC = posterior commissure

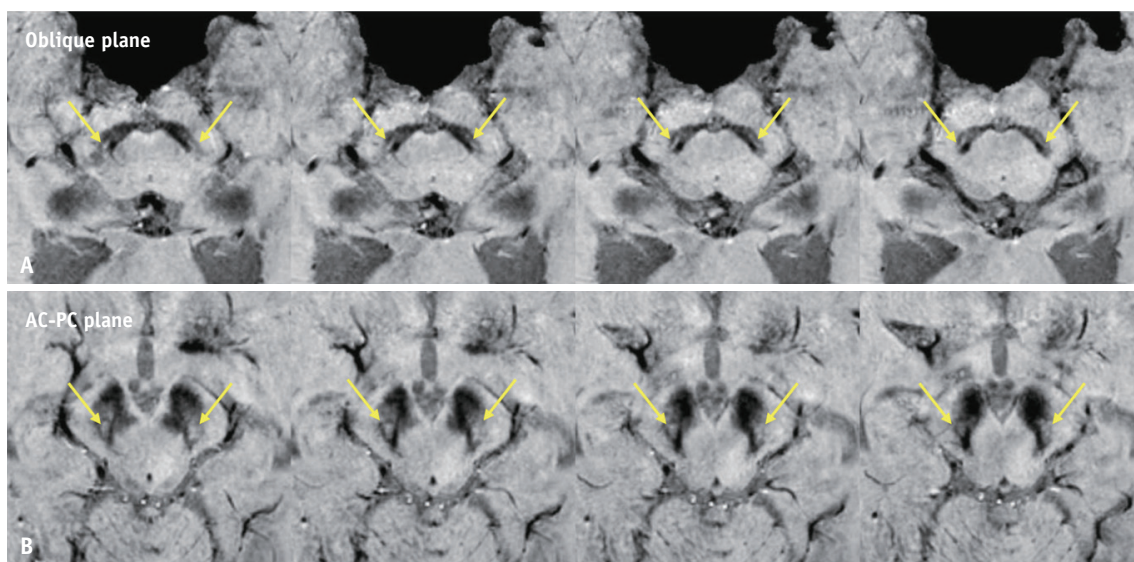


Fig. 3. Images both readers assessed as normal (grade 0) for both sides of the substantia nigra. The hyperintense substantia nigra are clearly shown in all four consecutive images immediately below the red nucleus in both (A) the oblique plane and (B) the AC-PC plane. Yellow arrows indicate the normal nigrosome 1 regions in the oblique and AC-PC planes, respectively. AC = anterior commissure, PC = posterior commissure

of the nigrosome 1 region; Category 1 was “probably abnormal,” indicating a partial or equivocal loss of the nigrosome 1 region; Category 0 was “normal,” indicating an intact nigrosome 1 region. Categories 1 and 2 were considered abnormal, and category 0 was considered normal; representative cases of each are shown in Figures 3 and 4.

The striatal dopamine transporter activity on ¹⁸F-FP-CIT PET was visually assessed according to previously published criteria [27]. Impaired presynaptic striatal dopamine

transporter density in any anatomical part of the striatum (dorsal posterior putamen, ventral putamen, and striatum) was considered abnormal. Each side of the basal ganglia was evaluated separately, and the presence or absence of an abnormality on each side was recorded. The presence or absence of hyperintensity in the substantia nigra on SMwI was compared with basal ganglia uptake on ¹⁸F-FP-CIT PET. Laterality was considered, considering the concurrent abnormalities between the SMwI and ¹⁸F-FP-CIT PET scans on

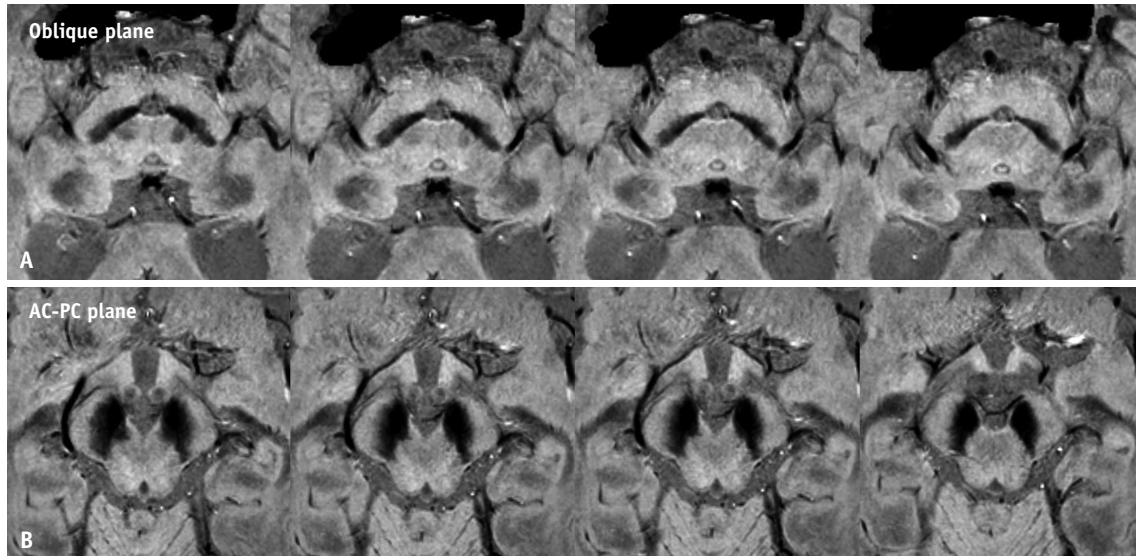


Fig. 4. Images both readers assessed as abnormal (grade 2) for both sides of the substantia nigra. The hyperintense areas in the hypointense substantia nigra are obliterated in all four consecutive images immediately below the red nucleus in both **(A)** the oblique plane and **(B)** the AC-PC plane. AC = anterior commissure, PC = posterior commissure

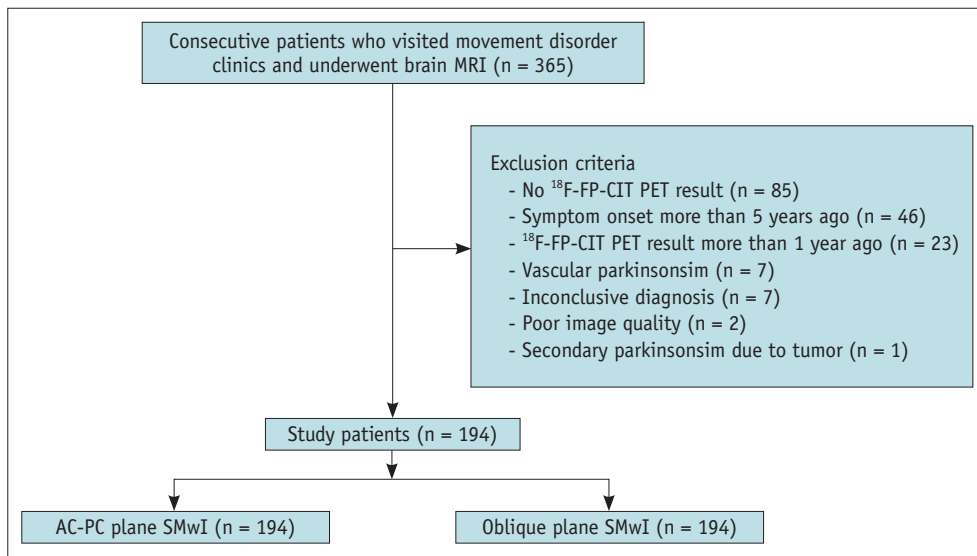


Fig. 5. Flowchart of the study selection process. ¹⁸F-FP-CIT = N-3-fluoropropyl-2-β-carbomethoxy-3-β-(4-iodophenyl) nortropone, AC = anterior commissure, PC = posterior commissure, SMwI = susceptibility map-weighted imaging

each side of the substantia nigra, for the evaluation of the diagnostic performance of SMwI.

QSM Analysis

For quantitative analysis of the nigrosome 1 region, we conducted additional analyses using QSM. First, two readers manually segmented the ROI of the normal nigrosome 1 region in the control group, which comprised 72 AC-PC and 79 oblique plane images. The averaged data for all nigrosome 1 masks were obtained by utilizing and

modifying the pipeline developed by Lancione et al. [28]. For measurement of the QSM values in the probabilistic nigrosome 1 ROI of each patient, the QSM-equivalent SMwIs were co-registered with the corresponding 3D-T1 weighted images. After converting the N1 probability binary mask generated in the normal group to QSM in the same space as the patient's SMwI, the average sensitivity (χ) for each subject was measured using the fslstats package in FSL on the QSM data, expressed in parts per million (ppm). A detailed description of the creation of the nigrosome 1

probability mask dataset and QSM value measurement is included in the Supplementary Materials and Supplementary Figure 1.

Statistical Analysis

Inter-rater agreement was assessed using Cohen's kappa coefficient. The diagnostic performances of the AC-PC plane and oblique coronal plane of SMwI were separately assessed for the left and right substantia nigra. This separation was done because asymmetric involvement of the substantia nigra is not uncommon in the early stage of IPD. We used the findings of ^{18}F -FP-CIT PET as the only reference standard for each side of the basal ganglia-substantia nigra, aside from the final clinical diagnosis. Multivariable logistic regression analysis with generalized estimating equations was applied to compare the sensitivity and specificity pooled across the two readers for the oblique and AC-PC planes. McNemar's test was used to compare the diagnostic performance between the two planes for each reader. Statistical significance was set at $P < 0.05$. All analyses were performed using the R software, version 3.6.3 (R Foundation for Statistical Computing, Vienna, Austria).

RESULTS

Clinical Characteristics

A total of 365 patients visited the movement disorder clinic and underwent brain MRI between September 2021 and December 2021. Patients with no ^{18}F -FP-CIT PET ($n = 85$), symptom onset more than 5 years ago ($n = 46$), ^{18}F -FP-CIT PET more than 1 year ago ($n = 23$), vascular Parkinsonism ($n = 7$), inconclusive diagnosis ($n = 7$), poor image quality ($n = 2$), or tumor Parkinsonism ($n = 1$) were excluded. A total of 194 patients (mean age \pm standard deviation, 67 ± 10 years, 91 male) were included (Fig. 5). The demographic and clinical characteristics of the patients are summarized in Table 1. Among them, 109 patients showed positive results on ^{18}F -FP-CIT PET, while 85 showed negative results. The mean age was 67 ± 10 and 68 ± 11 years for the ^{18}F -FP-CIT PET-positive and ^{18}F -FP-CIT PET-negative groups, respectively. The mean interval between the alleged disease onset and the MRI exam date was 1.0 ± 1.3 and 2.0 ± 2.0 years for the ^{18}F -FP-CIT PET-positive and ^{18}F -FP-CIT PET-negative groups, respectively. Of the entire patient cohort, 82 were diagnosed with IPD, 26 with multiple system atrophy, 3 with progressive supranuclear palsy, 10 with corticobasal degeneration, 35 with essential tremor, 10 with drug-induced parkinsonism, 4 with

Table 1. Demographic findings and clinical characteristics

Characteristic	PET positive (n = 109)	PET negative (n = 85)
Age, yr	67 ± 10	68 ± 11
Sex, male:female	56:53	35:50
Disease duration, yr	1.0 ± 1.3	2.0 ± 2.0

Data are mean \pm standard deviation or number of patients.

Table 2. Inter-rater agreement on oblique and AC-PC planes of SMwI

Side	Plane	Cohen's Kappa (95% CI)
Left	Oblique	0.772 (0.683–0.862)
	AC-PC	0.730 (0.634–0.827)
Right	Oblique	0.658 (0.552–0.764)
	AC-PC	0.741 (0.646–0.836)

AC = anterior commissure, PC = posterior commissure, SMwI = susceptibility map-weighted imaging, CI = confidence interval

idiopathic normal pressure hydrocephalus, and 24 with other conditions. The mean interval between MRI and ^{18}F -FP-CIT PET was 20.1 ± 47.3 days. The mean interval between the alleged date of disease onset and the MRI exam date was 27.1 ± 18.7 months.

Inter-Rater Agreement on Oblique and AC-PC Planes of SMwI

The inter-rater agreement was good for the oblique plane, both for the right ($\kappa = 0.658$) and the left ($\kappa = 0.772$) sides of the substantia nigra. The inter-rater agreement for the AC-PC plane was also good, both for the right ($\kappa = 0.741$) and the left ($\kappa = 0.730$) sides of the substantia nigra. The results are summarized in Table 2.

Diagnostic Performance of Oblique and AC-PC Planes of SMwI

The overall diagnostic performance pooled across the two readers and the individual readers' performances in the oblique and AC-PC planes are described in Table 3. When stratified by side, for the left side, the overall sensitivity of the oblique plane was 86.4% (178/206, 95% CI: 79.4%–91.3%), while that of the AC-PC plane was 87.4% (180/206; 95% CI: 81.0%–91.8%). In addition, for the left side, the overall specificity of the oblique plane was 83.5% (152/182, 95% CI: 75.8%–89.1%), while that of the AC-PC plane was 83.5% (152/182; 95% CI: 75.8%–89.1%). Conversely, for the right side, the overall sensitivity of the oblique plane was 83.3% (175/210, 95% CI: 76.4%–88.5%), while that of the AC-PC plane was 87.6% (184/210; 95% CI: 81.4%–92.0%).

Table 3. Diagnostic performance of SMwI for readers 1 and 2, stratified by side and plane

	Left			Right		
	Oblique	AC-PC	<i>P</i>	Oblique	AC-PC	<i>P</i>
Overall performance (pooled across readers)						
Sensitivity	86.4 (79.4, 91.3)	87.4 (81.0, 91.8)	0.695	83.3 (76.4, 88.5)	87.6 (81.4, 92.0)	0.079
Specificity	83.5 (75.8, 89.1)	83.5 (75.8, 89.1)	1	82.0 (74.4, 87.8)	86.0 (78.5, 91.1)	0.157
Accuracy	85.1 (80.1, 89.0)	85.6 (80.8, 89.3)	0.763	82.7 (77.8, 86.7)	86.9 (82.3, 90.4)	0.025
Reader 1						
Sensitivity	87.4 (81.0, 93.8)	91.3 (85.8, 96.7)	0.344	85.7 (79.0, 92.4)	87.6 (81.3, 93.9)	0.754
Specificity	86.8 (79.9, 93.8)	86.8 (79.9, 93.8)	1	86.5 (79.4, 93.6)	86.5 (79.4, 93.6)	1
Accuracy	87.1 (82.4, 91.8)	89.2 (84.8, 93.5)	0.481	86.1 (81.2, 91.0)	87.1 (82.4, 91.8)	0.815
Reader 2						
Sensitivity	85.4 (78.6, 92.2)	83.5 (76.3, 90.7)	0.791	81.0 (73.4, 88.5)	87.6 (81.3, 93.9)	0.143
Specificity	80.2 (72.0, 92.2)	80.2 (72.0, 92.2)	1	77.5 (68.9, 86.2)	85.4 (78.1, 92.7)	0.189
Accuracy	83.0 (77.7, 88.3)	82.0 (76.5, 87.4)	0.856	79.4 (73.7, 85.1)	86.6 (81.8, 91.4)	0.034

Data are presented with a 95% confidence interval.

SMwI = susceptibility map-weighted imaging, AC = anterior commissure, PC = posterior commissure

In addition, for the right side, the overall specificity of the oblique plane was 82.0% (146/178, 95% CI: 74.4%–87.8%), while that of the AC-PC plane was 86.0% (153/178; 95% CI: 78.5%–91.1%). There was no significant difference in sensitivity and specificity between the oblique and AC-PC planes for the left and right sides.

Multivariable logistic regression analysis with generalized estimating equations revealed no significant differences in sensitivity and specificity between the oblique and AC-PC planes. The odds ratio of sensitivity for the AC-PC plane was 1.25 (95% CI: 0.90–1.74; *P* = 0.182), and that of specificity for the AC-PC plane was 0.87 (95% CI: 0.63–1.19; *P* = 0.378).

QSM Analysis

The mean QSM value of the IPD group was significantly higher than that of the control group (Supplementary Fig. 2). The sensitivity and specificity of QSM values using the AC-PC plane for differentiating parkinsonism were 59.4% and 80.6%, respectively (Supplementary Fig. 3), while the corresponding values using the oblique plane were 60.4% and 72.2%, respectively (Supplementary Fig. 4).

DISCUSSION

The present study compared the diagnostic performance of the SMwI oblique plane and AC-PC plane in determining nigral hyperintensities in the substantia nigra. The inter-rater agreement was good for both the oblique and AC-PC planes, which both showed high sensitivity (86.4%/87.4%, and 83.3%/87.6%, left/right, respectively) and specificity

(83.5%/83.5% and 82.0%/86.0%, left/right, respectively) for determining nigral hyperintensities in the substantia nigra. In both analyses, there was no significant difference in diagnostic performance between the oblique and AC-PC planes.

Many previous studies have demonstrated the high diagnostic performance of SMwI in assessing nigral hyperintensity [8,12,16–18]. However, most previous studies were conducted with varying imaging protocols, and presented conflicting assumptions regarding the optimal imaging plane for assessing nigral hyperintensity [9,20]. Although a recent study proposed a standardized protocol for SMwI recommending the oblique plane as the preferred MR acquisition plane, it lacked a valid demonstration of the superiority of the oblique plane over other planes [16].

This study is the first to demonstrate no significant difference between the SMwI oblique plane and the AC-PC plane in determining nigral hyperintensity in the substantia nigra. This result is inconsistent with that of a recent meta-analysis suggesting that the type of MR acquisition plane was a source of heterogeneity in assessing nigral hyperintensity [13]. We assumed that this difference occurred because this meta-analysis included only SWI images and not SMwI images. The exceptional spatial resolution of SMwI might nullify the effect of the type of MR acquisition plane on the visualization of nigral hyperintensities. Many previous studies have advocated the use of SMwI over SWI as it enhances the contrast-to-noise ratio by reducing artifacts related to the magnetic field [9,20,29]. Kim et al. [20] showed that SMwI provided the highest contrast-to-noise ratio among five susceptibility-weighted contrasts (magnitude, phase,

QSM, SWI, and SMwI). However, they also insisted that the oblique coronal plane should be used rather than other types of planes because it can minimize the partial volume effects from neighboring substantia nigra structures. This could burden many institutions, as many have already adopted the AC-PC plane, which radiology technicians can generate relatively conveniently. However, our results suggest that the superiority of SMwI might surpass previous expectations to the extent that it can nullify the impact of the type of MR acquisition plane on the visualization of the nigrosome region. Our results thus affirm that each institution may choose one of the SMwI imaging planes between the oblique and AC-PC planes according to the clinical setting. This may reduce the concern regarding the type of MR acquisition plane to adopt, reducing the burden on each institution to change its preexisting MR protocols for the MR acquisition plane.

Furthermore, our results showed better accuracy than recent SMwI studies, which showed diagnostic accuracies ranging from 71.7% to 73.6% [8,12]. In our study, the accuracy of SMwI was 85.1%/82.7% (left/right) in the oblique plane and 85.6%/86.9% (left/right) in the AC-PC plane. We speculate that this is because previous studies produced images faster (30 slices; 3 minutes and 50 seconds using a 3T Philips scanner) than ours (32 slices; shortest TR using a 3T Philips scanner), indicating the possibility of under-sampling images and interfering with diagnostic accuracy. Furthermore, one notable aspect of our study was that, unlike previous investigations in which only experienced neuroradiologists with more than 10 years of experience were included [8,12,16], a radiologist with only 2 years of experience participated as Reader 2 in our study. This result suggests that even with a short training session, inter-rater agreement was high in the oblique and AC-PC planes. Oblique plane: $\kappa = 0.772/0.658$ (left/right), and AC-PC plane: $\kappa = 0.730/0.741$ (left/right). Moreover, reader 2 showed high accuracy in the oblique and AC-PC planes. Oblique plane: 83.0%/79.4% (left/right); and AC-PC plane: 82.0%/86.6% (left/right). This result implies that, even for a novice reader with little training, an accurate diagnosis of nigral hyperintensity is feasible using SMwI.

In addition, we conducted a quantitative analysis using QSM. The mean QSM value for the IPD group was statistically higher than that for the control group. However, the sensitivity and specificity of the QSM values obtained using AC-PC or oblique planes were lower than those obtained from the visual assessment of SMwI. We therefore speculate that these QSM results can be attributed to the current

lack of a settled protocol for generating and analyzing QSM [20,30,31]. Although QSM is expected to enable quantitative analysis of the nigrosome 1 region, there are still several limitations and obstacles for its universal implementation.

Our study has several limitations. First, the single-center design would have introduced the possibility of selection bias. However, to overcome this, we endeavored to reflect real-world data with a consecutive study design, including only subjects with early stage primary parkinsonism whose imaging acquisition was achieved within 5 years of symptom onset. By excluding patients with advanced-stage Parkinsonism, we prevented inflation of the effect of disease duration on MR images. Second, because we used only one type of MR scanner (Philips); thus, it might be challenging to draw a general conclusion regarding the usability of SMwI without comparison with other types of MR scanners. Moreover, a previous multicenter study which included subjects from 10 hospitals [16], revealed that the Philips scanner showed a lower diagnostic accuracy of 93.8% than the Siemens scanner of 98.4% for diagnosis of Parkinsonism with SMwI. However, in the previous study, a comparison was not conducted with the same images but with different images from different hospitals. Furthermore, as the author pointed out, this result may have been due to a high incidence of motion-induced artifacts in specific centers that used a Philips scanner. Conversely, only two of 365 consecutive patients in our study (0.5%) showed poor image quality with the Philips scanner among, compared with 1.1% (3/265) in a previous study. In addition, in clinical settings, Philips scanners are more commonly used to acquire SMwI images than Siemens scanners [13]. We believe that our numerical results and practical clinical situations can be supported using a Philips scanner to generate SMwI images, rather than other MR scanners.

Third, we compared only two MR acquisition planes among the four previously mentioned types. However, it appeared practically impossible to compare all types of MR planes. Because it took at least 5 minutes to acquire an oblique coronal SMwI image, it was not feasible to generate and interpret four different types of SMwI image planes for all included patients. In addition, as most hospitals and recent studies chose either to apply oblique coronal or AC-PC SMwI planes, while only a minority of hospitals and a few previous pioneering studies used other types of SMwI planes, it was uncertain whether there would be much practical value of the results, even if we conducted additional analyses with

other types of image planes. Therefore, we determined that comparing the AC-PC plane, the most commonly utilized plane, with the oblique plane, the plane most insusceptible to the partial volume effect, was both reasonable and practical. Overall, we assumed that similar results would be obtained with other MR planes if assessed with the same spatial resolution. Lastly, we only assessed the difference according to the imaging planes by unifying the echo time and slice thickness. Further studies with differing echo times and slice thicknesses in SMwI are warranted to evaluate nigral hyperintensities, as a previous meta-analysis demonstrated that these could be sources of heterogeneity [13].

In conclusion, the present study indicated that there are no significant difference in the diagnostic performance of SMwI performed in the oblique and AC-PC plane in discriminating patients with parkinsonism from those without. This finding affirms that each institution may choose the imaging plane for SMwI according to their clinical settings.

Supplement

The Supplement is available with this article at <https://doi.org/10.3348/kjr.2023.0920>.

Availability of Data and Material

The datasets generated or analyzed during the study are available from the corresponding author on reasonable request.

Conflicts of Interest

Chong Hyun Suh and Ho Sung Kim, who hold respective positions on the Assistants to the Editor and Section Editor of the *Korean Journal of Radiology*, were not involved in the editorial evaluation or decision to publish this article. The remaining author has declared no conflicts of interest.

Author Contributions

Conceptualization: Chong Hyun Suh, Eung Yeop Kim. Data curation: Suiji Lee, Chong Hyun Suh, Hwon Heo, Woo Hyun Shim. Formal analysis: Suiji Lee, Chong Hyun Suh, Hwon Heo, Woo Hyun Shim. Funding acquisition: Chong Hyun Suh, Eung Yeop Kim. Investigation: Chong Hyun Suh, Eung Yeop Kim. Methodology: Chong Hyun Suh, Eung Yeop Kim. Project administration: Chong Hyun Suh, Eung Yeop Kim. Resources: Sungyang Jo, Sun Ju Chung. Software: Hwon Heo, Woo Hyun Shim, Jongho Lee. Supervision: Eung Yeop Kim, Sang Joon Kim. Validation: Chong Hyun Suh, Hwon

Heo. Visualization: Suiji Lee, Chong Hyun Suh, Hwon Heo. Writing—original draft: Suiji Lee. Writing—review & editing: all authors.

ORCID IDs

Suiji Lee

<https://orcid.org/0009-0001-1301-6461>

Chong Hyun Suh

<https://orcid.org/0000-0002-4737-0530>

Sungyang Jo

<https://orcid.org/0000-0001-5097-2340>

Sun Ju Chung

<https://orcid.org/0000-0003-4118-8233>

Hwon Heo

<https://orcid.org/0000-0002-6103-4680>

Woo Hyun Shim

<https://orcid.org/0000-0002-7251-2916>

Jongho Lee

<https://orcid.org/0000-0001-9602-2244>

Ho Sung Kim

<https://orcid.org/0000-0002-9477-7421>

Sang Joon Kim

<https://orcid.org/0000-0001-7070-7333>

Eung Yeop Kim

<https://orcid.org/0000-0002-9579-4098>

Funding Statement

This work was supported by the National Research Foundation of Korea (NRF-2021R1C1C1014413 and NRF-2022R1F1A1073551). We thank the Biomedical Computing core facility at the ConveRgence mEDicine research cenTer (CREDIT), Asan Medical Center for their technical support and instrumentation.

REFERENCES

- Gibb WR, Lees AJ. The relevance of the Lewy body to the pathogenesis of idiopathic Parkinson's disease. *J Neurol Neurosurg Psychiatry* 1988;51:745-752
- Postuma RB, Berg D, Stern M, Poewe W, Olanow CW, Oertel W, et al. MDS clinical diagnostic criteria for Parkinson's disease. *Mov Disord* 2015;30:1591-1601
- Cosottini M, Frosini D, Pesaresi I, Costagli M, Biagi L, Ceravolo R, et al. MR imaging of the substantia nigra at 7 T enables diagnosis of Parkinson disease. *Radiology* 2014;271:831-838
- Schwarz ST, Afzal M, Morgan PS, Bajaj N, Gowland PA, Auer DP. The 'swallow tail' appearance of the healthy nigrosome - a new accurate test of Parkinson's disease: a case-control and retrospective cross-sectional MRI study at 3T. *PLoS One*

- 2014;9:e93814
5. Gao P, Zhou PY, Li G, Zhang GB, Wang PQ, Liu JZ, et al. Visualization of nigrosomes-1 in 3T MR susceptibility weighted imaging and its absence in diagnosing Parkinson's disease. *Eur Rev Med Pharmacol Sci* 2015;19:4603-4609
 6. Noh Y, Sung YH, Lee J, Kim EY. Nigrosome 1 detection at 3T MRI for the diagnosis of early-stage idiopathic Parkinson disease: assessment of diagnostic accuracy and agreement on imaging asymmetry and clinical laterality. *AJNR Am J Neuroradiol* 2015;36:2010-2016
 7. Stezin A, Naduthota RM, Botta R, Varadharajan S, Lenka A, Saini J, et al. Clinical utility of visualisation of nigrosome-1 in patients with Parkinson's disease. *Eur Radiol* 2018;28:718-726
 8. Bae YJ, Song YS, Choi BS, Kim JM, Nam Y, Kim JH. Comparison of susceptibility-weighted imaging and susceptibility map-weighted imaging for the diagnosis of parkinsonism with nigral hyperintensity. *Eur J Radiol* 2021;134:109398
 9. Nam Y, Gho SM, Kim DH, Kim EY, Lee J. Imaging of nigrosome 1 in substantia nigra at 3T using multiecho susceptibility map-weighted imaging (SMWI). *J Magn Reson Imaging* 2017;46:528-536
 10. Kim EY, Sung YH, Shin HG, Noh Y, Nam Y, Lee J. Diagnosis of early-stage idiopathic Parkinson's disease using high-resolution quantitative susceptibility mapping combined with histogram analysis in the substantia nigra at 3 T. *J Clin Neurol* 2018;14:90-97
 11. Gho SM, Liu C, Li W, Jang U, Kim EY, Hwang D, et al. Susceptibility map-weighted imaging (SMWI) for neuroimaging. *Magn Reson Med* 2014;72:337-346
 12. Bae YJ, Song YS, Kim JM, Choi BS, Nam Y, Choi JH, et al. Determining the degree of dopaminergic denervation based on the loss of nigral hyperintensity on SMWI in parkinsonism. *AJNR Am J Neuroradiol* 2021;42:681-687
 13. Kim PH, Lee DH, Suh CH, Kim M, Shim WH, Kim SJ. Diagnostic performance of loss of nigral hyperintensity on susceptibility-weighted imaging in parkinsonism: an updated meta-analysis. *Eur Radiol* 2021;31:6342-6352
 14. Mitchell T, Lehericy S, Chiu SY, Strafella AP, Stoessl AJ, Vaillancourt DE. Emerging neuroimaging biomarkers across disease stage in Parkinson disease: a review. *JAMA Neurol* 2021;78:1262-1272
 15. Liu X, Wang N, Chen C, Wu PY, Piao S, Geng D, et al. Swallow tail sign on susceptibility map-weighted imaging (SMWI) for disease diagnosing and severity evaluating in parkinsonism. *Acta Radiol* 2021;62:234-242
 16. Sung YH, Kim JS, Yoo SW, Shin NY, Nam Y, Ahn TB, et al. A prospective multi-centre study of susceptibility map-weighted MRI for the diagnosis of neurodegenerative parkinsonism. *Eur Radiol* 2022;32:3597-3608
 17. Sung YH, Lee J, Nam Y, Shin HG, Noh Y, Hwang KH, et al. Initial diagnostic workup of parkinsonism: dopamine transporter positron emission tomography versus susceptibility map-weighted imaging at 3T. *Parkinsonism Relat Disord* 2019;62:171-178
 18. Wang N, Liu XL, Li L, Zuo CT, Wang J, Wu PY, et al. Screening for early-stage Parkinson's disease: swallow tail sign on MRI susceptibility map-weighted images compared with PET. *J Magn Reson Imaging* 2021;53:722-730
 19. Cosottini M, Frosini D, Pesaresi I, Donatelli G, Cecchi P, Costagli M, et al. Comparison of 3T and 7T susceptibility-weighted angiography of the substantia nigra in diagnosing Parkinson disease. *AJNR Am J Neuroradiol* 2015;36:461-466
 20. Kim EY, Sung YH, Lee J. Nigrosome 1 imaging: technical considerations and clinical applications. *Br J Radiol* 2019;92:20180842
 21. Shin DH, Heo H, Song S, Shin NY, Nam Y, Yoo SW, et al. Automated assessment of the substantia nigra on susceptibility map-weighted imaging using deep convolutional neural networks for diagnosis of idiopathic Parkinson's disease. *Parkinsonism Relat Disord* 2021;85:84-90
 22. Bossuyt PM, Reitsma JB, Bruns DE, Gatsonis CA, Glasziou PP, Irwig L, et al. STARD 2015: an updated list of essential items for reporting diagnostic accuracy studies. *BMJ* 2015;351:h5527
 23. Armstrong MJ, Litvan I, Lang AE, Bak TH, Bhatia KP, Borroni B, et al. Criteria for the diagnosis of corticobasal degeneration. *Neurology* 2013;80:496-503
 24. Bhatia KP, Bain P, Bajaj N, Elble RJ, Hallett M, Louis ED, et al. Consensus statement on the classification of tremors. From the task force on tremor of the International Parkinson and Movement Disorder Society. *Mov Disord* 2018;33:75-87
 25. Gilman S, Wenning GK, Low PA, Brooks DJ, Mathias CJ, Trojanowski JQ, et al. Second consensus statement on the diagnosis of multiple system atrophy. *Neurology* 2008;71:670-676
 26. Höglinger GU, Respondek G, Stamelou M, Kurz C, Josephs KA, Lang AE, et al. Clinical diagnosis of progressive supranuclear palsy: the movement disorder society criteria. *Mov Disord* 2017;32:853-864
 27. Tatsch K, Poepperl G. Nigrostriatal dopamine terminal imaging with dopamine transporter SPECT: an update. *J Nucl Med* 2013;54:1331-1338
 28. Lancione M, Donatelli G, Del Prete E, Campese N, Frosini D, Cencini M, et al. Evaluation of iron overload in nigrosome 1 via quantitative susceptibility mapping as a progression biomarker in prodromal stages of synucleinopathies. *Neuroimage* 2022;260:119454
 29. Bae YJ, Kim JM, Sohn CH, Choi JH, Choi BS, Song YS, et al. Imaging the substantia nigra in Parkinson disease and other Parkinsonian syndromes. *Radiology* 2021;300:260-278
 30. Pyatigorskaya N, Sanz-Morère CB, Gaurav R, Biondetti E, Valabregue R, Santin M, et al. Iron imaging as a diagnostic tool for Parkinson's disease: a systematic review and meta-analysis. *Front Neurol* 2020;11:366
 31. Mazzucchi S, Frosini D, Costagli M, Del Prete E, Donatelli G, Cecchi P, et al. Quantitative susceptibility mapping in atypical parkinsonisms. *Neuroimage Clin* 2019;24:101999